This is a post-peer-review version of an article published in I**nfrared Physics & Technology,** Volume 111, 2020, 103481. The final authenticated version is available online at:

https://doi.org/10.1016/j.infrared.2020.103481

I. Garrido, S. Lagüela, R. Otero, P. Arias. Thermographic methodologies used in infrastructure inspection: A review—data acquisition procedures, Infrared Physics & Technology, Volume 111, 2020, 103481

THERMOGRAPHIC METHODOLOGIES USED IN INFRASTRUCTURE INSPECTION: A REVIEW—DATA ACQUISITION PROCEDURES

I. Garrido*[1], S. Lagüela[2], R. Otero[1] and P. Arias[1]

[1] Universidade de Vigo, Centro de Investigación en Tecnoloxías, Enerxía e Procesos Industriais (CINTECX), Applied Geotechnologies Research Group, Campus Universitario de Vigo, As Lagoas, Marcosende, 36310 Vigo (Spain)

[2] Department of Cartographic and Terrain Engineering, University of Salamanca, EPS Ávila, Calle Hornos Caleros 50, 05003 Ávila (Spain)

***Corresponding author:** ivgarrido@uvigo.es; **+34 986 813 499**

Abstract

InfraRed Thermography (IRT) is one of the best tools for the thermal characterization of the materials of structures and for the detection and thermal characterization of the most typical defects in the infrastructure field. An exhaustive review of the most recent thermographic acquisition (data collection) procedures in infrastructure inspection is presented here, comparing the existing variety of experimental thermographic configurations for infrastructure inspection. Furthermore, a discussion searching similarities and differences between data collection procedures, together with a series of objective and critical conclusions, are described.

Keywords: infrared thermography, data acquisition, infrastructure, inspection, review

1. Introduction

Over the years, the continuous deterioration of any type of infrastructure is a real fact. Therefore, it is important to maintain these structures in good condition, due to their important role in the lives of the people:

1) Residential and public/private service buildings allow people to live in.

2) Bridges, roads and airports allow the movement from one place to another, ensuring communication and promoting evolution.

3) Sites of great heritage value, such as panels or stone sculptures, stand as key features in the history of humanity.

The importance of maintenance activities in infrastructures is shown in the section “Implementing Operations & Maintenance Best Practices” of the World Economic Forum’s Strategic Infrastructure 2014 report [1]. Specifically, it indicates the need to perform the most appropriate measures of prevention and maintenance, on a regular basis, for each of the infrastructures during their lifetimes. To this end, the application of the best techniques for assessing and tracking infrastructure integrity is an adequate solution. In other words, the detection and characterization of the nature of possible defects in an

infrastructure must be performed with the least harmful, fastest and most accurate tools [2].

The techniques most traditionally used as assessing and tracking tools are not able to detect the extent of defects of an infrastructure with good accuracy, since they are mainly based on visual and subjective observations [3]. For example, the method of the sounding hammer and chain drag can locate delaminated regions in bridge slabs by comparing the resonating sounds of the defected and undamaged areas [4]. Moreover, these methods only indicate the presence of a defect in the structure under study [2] and cannot be used for quantitative analysis. In this way, only qualitative studies are possible, without being able to quantify any thermophysical or structural parameter of the infrastructure and its possible defects.

Thus, in the last years, Non-Destructive Techniques (NDTs) have emerged as new technologies for the inspection of different infrastructures [3], not only to improve the qualitative analysis, but also to assess each structure quantitatively. According to [5], NDTs are attractive and useful to determine ductility and impact resilience, fatigue strength and fracture in the materials under study, among others. Indeed, according to Miskiewicz et al. [6], NDTs are being increasingly used in structural health monitoring and technical state evaluation. Unlike destructive techniques, the main feature of NDTs is that they do not intrude upon or affect the structure analysed in any way. Besides, most NDTs work without contact. This fact allows the performance of the evaluation of objects with difficult access or dangerous properties from a safety distance.

In addition, an NDT inspection avoids the subjectivity and slowness of traditional methods [7].

The names of the different NDTs often refer to the type of signal or to the equipment used. According to the American Society for Non-Destructive Testing (ASNT), there are 16 different NDTs [8]. For instance, Acoustic Emission (AE) is one of the NDTs used in the infrastructure field where a localized external force, such as abrupt mechanical loads, rapid temperature or pressure changes, is applied. Thus, it is possible to assess the deformation of buried infrastructures through the resulting stress waves [9]. Another NDT is Electromagnetic Testing (ET), which includes Eddy Current Testing (ECT), Alternating Current Field Measurement (ACFM) and Remote Field Testing (RFT). All these techniques use the induction of an electric current or magnetic field in a conductive part of the structure under study for the analysis of the resulting effects. Among works with this tool, Sun et al. [10] propose a novel electromagnetic technique for the health monitoring of a concrete bar. Additionally, Guided Wave Testing (GWT) uses controlled excitation of one or more ultrasonic waveforms that travel along the length of a metallic structure, analysing the reflected waves. For instance, Evans et al. [11] describe the applicability of the GTW to the inspection of level crossing rails. Other common NDTs in the infrastructure field are Ground Penetrating Radar (GPR) and Laser Testing Method (LTM). The first technique consists of using radar pulses to obtain information of the interior of the structure under study, in two-dimensional image format (2D). For this purpose, electromagnetic radiation in the microwave band is applied to the structure, and the reflected signals are detected and analysed. Among GPR case studies,

Prego et al. [12] show a new GPR signal processing tool for mobile devices to measure thickness and diameters in rebar or piping. Regarding LTM, this technique includes three different tools: holography, shearography and profilometry. All of them use laser to perform the inspections. With the first method, Sfarra et al. [13] validate the effectiveness of an integrated approach using, among others, the holography technique to discover old repairs and/or inclusions of foreign materials in a wooden structure. In addition, Buchta et al. [14] investigate the combination of the finite element method with shearography for the defect detection on artwork, and Martínez-Sánchez et al. [15] integrate different instrumentation and sensors, including a laser profilometer, in a Mobile Mapping (MM) vehicle for the continuous record of quantitative data suitable for roadside inspection.

The combination of different technologies enriches their individual use. This is shown by Lagüela et al. [16] and Puente et al. [17], among others, who combine GPR with other NDTs, such as InfraRed Thermography (IRT) and Terrestrial Light Detection And Ranging (T-LiDAR), for the detection of damage in pavement and for the three-dimensional (3D) reconstruction of an archaeological site, respectively.

Therefore, NDTs provide a wide range of knowledge of infrastructures, from their characterization as a whole and by component, to the detection and characterization of surface and subsurface defects. Among all NDTs, IRT is one of the most widely used and accepted technology for the thermal

characterization of infrastructures, allowing the identification and thermal analysis of defects, such as:

1) Thermal bridges or air infiltration in buildings.

2) Cracks and moisture in any type of infrastructure, located both superficially and internally in the structures.

These defects cause an anomalous temperature distribution in their areas with regard to the temperature distribution in the unaltered zones [18]. This is due to the different movement of fluids through the construction elements and through the defects [19]. Given that IRT measures the surface temperature of the objects, it is possible to:

1) Detect (qualitative analysis) and thermally characterize the different defects (quantitative analysis) during the data post-acquisition stage.

2) Perform the thermal characterization of the structure under study (quantitative analysis) during the data post-acquisition stage.

In addition, IRT gives the temperature measurements with:

1) High accuracy.

2) In a non-contact manner.

3) In real time.

4) With high scanning-speed.

5) In 2D image format.

6) Without emitting any harmful radiation.

Thus, there are many applications with this technique, alone or in combination with other NDTs that complement the capabilities of penetration lacking for IRT, as seen in [16,17].

Despite the long history of the IRT technique, with the first camera invented in 1929 [20], IRT studies continue to propose new methods, improving the results of this tool and expanding its fields of application. Proof of this are the recent reviews on IRT published [18,20–28]. Bagavathiappan et al. [18] study the advances of IRT on condition monitoring of machinery, equipment and processes. Kylili et al. [20] describe the fields of application of IRT in the building sector, while Lucchi [21] presents a procedure for the energy audit applying IRT. Vavilov and Burleigh [22] summarize the fundamentals of one of the IRT data acquisition procedures and its applications in the aerospace industry, and Yang and He [23] review the IRT data acquisition procedures for composites inspection. Garrido et al. [24,25] study several IRT applications for infrastructure inspection and review the most recent thermographic procedures for infrastructure applications, focusing on the data post-acquisition stage, respectively. Nardi et al. [26] compare IRT with the common approaches for the overall heat transfer coefficient evaluation and Kirmtat & Krejcar [27] also show the utility of IRT in buildings. Usamientaga et al. [28] explain the common IRT procedures for temperature measurement and Non-Destructive Testing in various industrial fields. All of them are exhaustive reviews but there is a lack of an in-depth analysis regarding the most recent IRT data acquisition procedures

covering the three main areas in the field of infrastructures in a single review, defined these procedures as the stages of thermal image acquisition without considering the subsequent thermal image processing/data post-acquisition stage. The three main areas in the field of infrastructures are: civil infrastructures, heritage sites and buildings. Then, this review paper describes the most current thermographic data acquisition procedures used in the infrastructure field, taking into account the main structure groups. Specifically, Fig. 1 shows the structure of the review.

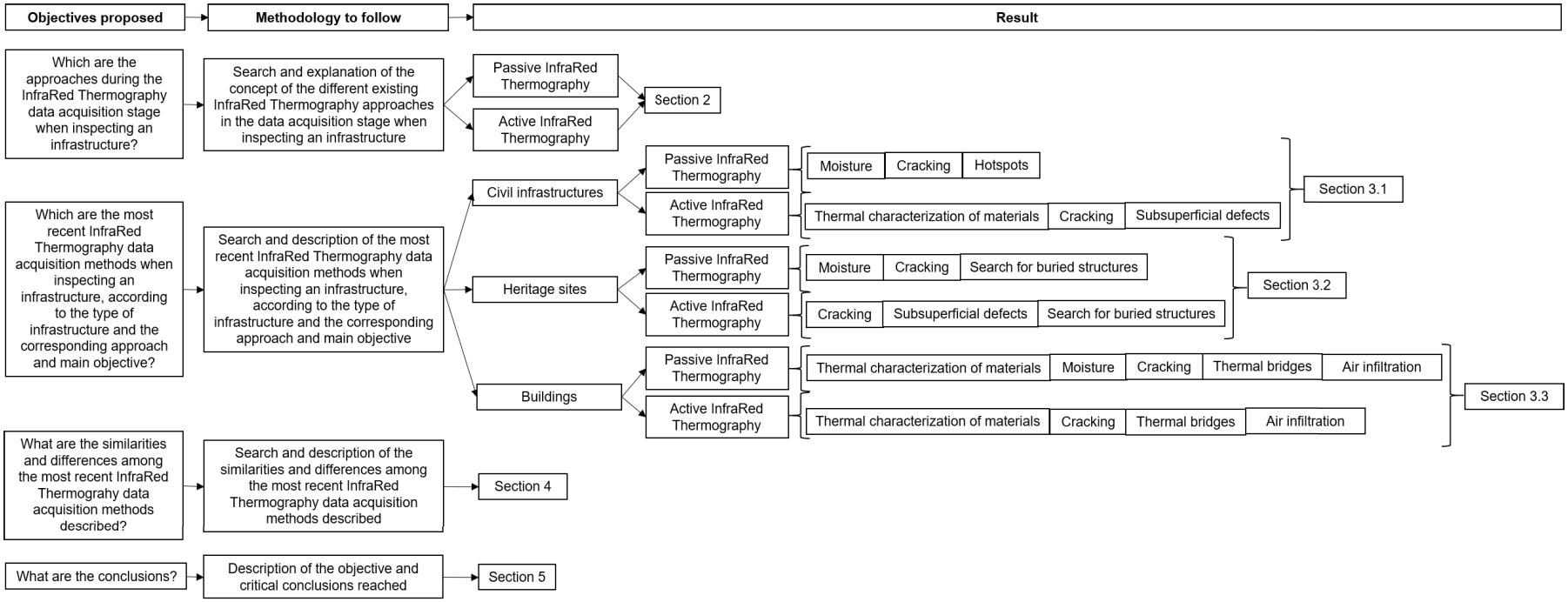

Fig. 1. Structure of contents in this review paper.

2. IRT approaches for data collection

When the inspection of an infrastructure is performed with IRT, two possible approaches can be applied for the data acquisition stage: passive and active IRT [29]. These are differentiated based on the absence or presence of an artificial external heat stimulation applied to the surface of the structure under study.

If the surface of the infrastructure is inspected using an InfraRed (IR) camera with a natural external heat source, typically solar radiation [30], the corresponding data acquisition approach is passive IRT. The natural thermal behaviour of the structure is captured through the thermal images acquired with the IR camera [31] because the structure under study is under real conditions during the measurements.

On the other hand, although passive IRT is often associated with building applications [32], or other types of infrastructure, due to its better suitability for inspecting large areas, there are also IRT works that use artificial external heat stimulations. This data acquisition approach is known as active IRT. In this type of data acquisition, the IR camera measures the heating and/or cooling processes of the surface of the infrastructure during and/or after the thermal stimulation [33]. The active IRT approach is used with the objective of producing a higher thermal contrast in the thermal images with regard to the results that would be obtained with passive IRT, which is necessary to:

1) Perform a more accurate thermal characterization of the defects [32].

2) Increase the visibility of possible subsurface defects [28,31].

The different artificial external thermal stimulations used in the infrastructure field can be classified as follows [23,24]:

1) Traditional techniques: Heat gun, hot water jets, hot air jets and hot water bag.

2) Optical heat sources: Flash and halogen lamps (optical thermography), and laser beam (laser thermography). The heating principle is based on optical-thermal effect, improving the defect detection rate of the traditional techniques.

3) Advanced techniques: The new thermal sources most commonly used in the infrastructure field are eddy current/induction thermography, microwave thermography and ultrasound thermography. The heating principle of the eddy current/induction, microwave and ultrasound thermography is the Joule heating/eddy current loss, dielectric loss and friction, respectively. The first technique uses induced eddy current as thermal source to heat conductive materials, with differences between the heat produced/temperature increased by the Joule effect in the areas with defects and the unaltered zones of the analysed structure. The second method also uses electromagnetic excitation as thermal source, specifically microwave for dielectric materials, in order to detect defects according to the amount of heat generated. Finally, ultrasound thermography is one of the variants of vibrothermography and consists of the physical contact with the surface of the structure under study, by means of a sonotrode. The sonotrode excites the material with ultrasonic excitation,

generating three-dimensional vibrations that travel through the material and consequently generate the distribution of heat.

In addition, within active IRT, there are two types of subclassifications:

1) Depending on the relative positions of the IR camera and the artificial external heat source with regard to the surface of the structure under study.

2) Depending on the type of heating process.

In the first subclassification, the relative positions between the IR camera and the heat stimulation can be [23]:

1) At the same side with regard to the analysed infrastructure: Reflection mode.

2) At opposite sides with regard to the analysed infrastructure: Transmission mode.

The name of reflection mode is referred to the fact that the radiation received by the IR camera is mostly the reflected fraction, since the time difference between the heating and the thermal image acquisition does not allow the radiation transmitted through the structure to be received by the IR camera. The reflection mode is suitable for the analysis of surfaces of structures with a high emissivity value or superficial/subsuperficial defects with low depth. On the contrary, transmission mode is based on the application of the heating from one side, and the thermal image acquisition of the response of the structure from the other side, with the main objective of studying the emitted radiation through the

structure. It is adequate for the analysis of surfaces of infrastructures with a low emissivity value or subsuperficial defects with high depth.

In the second subclassification, the most common types of heating processes in the infrastructure field are the following, from the simplest to the most complex [28,34]:

1) Conventional Thermography (CT) or step heating.

2) Pulsed Thermography (PT).

3) Lock-in Thermography (LT).

CT consists of heating the surface of the structure to be studied in a continuous mode, analysing its thermal response [35]. Then, the data post-acquisition stage will consist of studying whether there is an unusual behaviour in the temperature evolution corresponding to a thermal irregularity or defect, by the application of different thermal image processing procedures.

When a short pulse of thermal stimulation is applied to the structure under study, with a duration from a few milliseconds to a few seconds [5], the type of heating process corresponds to PT. In this specific case, the decay curve of the temperature is investigated during the data post-acquisition stage [36–38], with a fast change of the surface temperature of the material while the thermal front is propagated by diffusion through the surface. Since the presence of deep discontinuities reduces the diffusion rate, it is possible to increase the visibility and perform a more accurate thermal characterization of defects at a certain depth [28].

If the surface of the infrastructure is modularly heated by a lock-in module, a sequence of temperature oscillations or thermal waves are generated on the surface under study. This type of heating process is known as LT. To do this heating, it is important to synchronize the IR camera with the heat source, studying the amplitude and phase of the measured thermal waves during the data post-acquisition stage [39]. Through the previous study, the thermal information on a superficial defect and the depth and thermal information on a subsuperficial defect can be obtained by analysing the phase delay [40] or the amplitude signatures [41].

3. Thermographic procedures in infrastructure inspections. Data acquisition stage

Since each type of infrastructure, and its possible types of defects, provide a different thermal response during the data acquisition stage of an IRT study [28], both in passive and active IRT, different data acquisition procedures are applied. The most recent IRT studies in infrastructure inspection are shown together with the data acquisition procedures according to:

1) The type of infrastructure (civil infrastructures/heritage sites/buildings).

2) The corresponding data acquisition approach (passive/active IRT).

3) The main objective of the inspection (thermal characterization of materials/defect analysis/search of buried structures).

Specifically, the following subsections cover one of the main groups of infrastructures, developing a table for each main objective that describes the following topics:

1) Experimental setup.

2) Infrastructure under study.

3) Type of IRT data acquisition.

It should be noted that the initials MWIR and LWIR used in the tables refer to Mid-Wave InfraRed and Long-Wave InfraRed, respectively. In addition, the symbols of T_{refl}, T_{atm} and RH_{atm} used in the tables stand for reflected temperature, atmospheric temperature and atmospheric relative humidity, respectively.

3.1. Civil infrastructures

Table 1 describes four recent IRT studies that thermally characterize materials within civil infrastructures. Specifically, all the IRT works included focus on the calculation of the thermal diffusivity parameter.

Work [Ref.]	Experimental setup	Infrastructure under study	Type of IRT data acquisition
Venegas et al. [42]	- Laboratory conditions: T_{refl} at 25 ºC, T_{atm} at 27ºC and RH_{atm} at 40% - Two halogen lamps of 1,000 W at 80% capacity - Test campaign: 10 s to heating, 10 s to cooling - IR camera spectral band/thermal image resolution: MWIR/320x256 pixels - Camera-to-object distance/angle with regard to the perpendicular of the object: 1.2 m/0º	Composites with thin inclusions, extrapolated to infrastructure scale	Active IRT: Optical thermography, CT, reflection mode and under laboratory conditions

	- Thermal stimulator-to-object distance/angle with regard to the perpendicular of the object: 0.9 m/35º - Thermal image acquisition frequency: Only during the cooling		
Balageas & Roche [43]	- Two flash lamps of a total of 6 kJ pulse energy - Test campaign: Heating of 4 ms, 299.996 s cooling - IR camera spectral band/thermal image resolution: MWIR/640x512 pixels - Thermal image acquisition frequency: 100 Hz, calculating the mean each 30x30 pixel zone	5.24 mm-thick plate made of carbon-epoxy, extrapolated to infrastructure scale	Active IRT: Optical thermography, PT, reflection/transmission mode and under laboratory conditions
Gnessougou et al. [44]	- Two flash lamps of 6.2 kJ pulse energy each lamp	Burnt and unburnt carbon fiber reinforced polymer materials with 1	Active IRT: Optical thermography, PT,

	- Test campaign: Heating of 2 ms, cooling less than 1 min - IR camera spectral band/thermal image resolution: MWIR/640x512 pixels	@ 2 cm-thick, extrapolated to infrastructure scale	transmission mode and under laboratory conditions
Kalyanavalli et al. [45]	1) In-depth thermal diffusivity: - Flash lamp of 6 kJ pulse energy - Test campaign: Heating for 2 ms, cooling for 19.998 s - IR camera spectral band/thermal image resolution: MWIR/320x256 pixels - Camera-to-object angle with regard to the perpendicular of the object: 0º - Thermal stimulator-to-object angle with regard to the perpendicular of the object: 0º	Basalt fiber reinforced composite, extrapolated to infrastructure scale	Active IRT: Optical thermography, PT and transmission mode (in-depth thermal diffusivity) Optical thermography, PT and transmission/reflection mode (in-plane thermal diffusivity) Under laboratory conditions

	- Thermal image acquisition frequency: 50 Hz 2) In-plane thermal diffusivity: - A halogen lamp of 1 kW, placing in front a circular aperture. The light is focused using a convex lens - Test campaign: Heating with a light spot of radius about 5 mm. Heating duration of 2 s (reflection mode) and 4 s (transmission mode), and cooling duration of 20 s - Camera-to-object distance/angle with regard to the perpendicular of the object: 0.35 m/0º - Thermal stimulator-to-object angle with regard to the perpendicular of the object: 0º

Table 1. Comparative table of the most recent IRT works related to the thermal characterization of materials within civil infrastructures. Specifically, all the IRT works included focus on the calculation of the thermal diffusivity parameter.

Table 2 describes four recent IRT studies that analyse moisture within civil infrastructures.

Work [Ref.]	Experimental setup	Infrastructure under study	Type of IRT data acquisition
Garrido et al. [46]	- Outdoor conditions: T_{atm} at 9 ºC and RH_{atm} at 90% - Indoor conditions: T_{atm} at 19 ºC and RH_{atm} at 40% - IR camera spectral band/thermal image resolution: LWIR/320x240 (for the beech pieces) and 640x480 (for the pillar) pixels - Camera-to-object distance/angle with regard to the perpendicular of the object: ≤10 m/≤ 50º	Beech pieces (indoor), extrapolated to infrastructure scale, and concrete pillar of a bridge (outdoor)	Passive IRT: Steady conditions and from outdoor and indoor

	- Thermal image acquisition frequency: One single thermal image		
Bach & Kodikara [47]	- Outdoor conditions: Between 4 a.m. and 6 a.m. - Test campaign: Before sunrise and in different months - IR camera spectral band/thermal image resolution: LWIR/240x180 pixels - Camera-to-object distance: 1 m @ 10 m	Small diameter buried reticulation pipes	Passive IRT: Steady conditions and from outdoor
Barreira et al. [48]	- Climatic chamber under stable conditions (T_{atm} and RH_{atm}): 19.5 ºC @ 20.5 ºC, 58% @ 62% - Test campaign: The specimen is partially humidified by the bottom surface, after being previously	A lightweight concrete specimen, extrapolated to infrastructure scale	Passive IRT: Steady conditions and from indoor

	dried in an oven. Thermal images acquisition starts from the beginning of the humidification process - IR camera spectral band/thermal image resolution: LWIR/320x240 pixels - Thermal image acquisition frequency: 0.0033 Hz for the first 8h, 0.0017 Hz for the remaining 16h		
Solla et al. [49]	- T_{atm} at 16 ºC and RH_{atm} at 70% - Test campaign: During the morning, with the incident solar radiation increasing during the survey	Inner roof surfaces of a military battery	Passive IRT: Steady conditions and from outdoor

	- IR camera spectral band/thermal image resolution: LWIR/640x480 pixels - Camera-to-object distance: 1 m - Thermal image acquisition frequency: One single thermal image		

Table 2. Comparative table of the most recent IRT works related to the analysis of moisture within civil infrastructures.

Table 3 describes seven recent IRT studies that analyse cracking within civil infrastructures.

Work [Ref.]	Experimental setup	Infrastructure under study	Type of IRT data acquisition
Solla et al. [49]	- T_{atm} at 16 ºC and RH_{atm} at 70% - Test campaign: During the morning, with the incident solar radiation increasing during the survey	Inner roof surfaces of a military battery	Passive IRT: Steady conditions and from outdoor

	- IR camera spectral band/thermal image resolution: LWIR/640x480 pixels - Camera-to-object distance: 1 m - Thermal image acquisition frequency: One single thermal image		
Solla et al. [50]	- Outdoor conditions: T_{atm} and RH_{atm} at 22 ºC and 41%, respectively - Test campaign: Before sunrise, on a cloudy day with no direct sun on the surface, and no rain - IR camera spectral band/thermal image resolution: LWIR/640x480 pixels	Asphalt pavement	Passive IRT: Steady conditions and from outdoor

	- Camera-to-object distance/angle with regard to the perpendicular of the object: 1 m/0º		
Rodríguez-Martín et al. [51]	- Electric heater with 2,500 W - Test campaign: 1) Toe crack: (20+10) min heating + cooling 2) Longitudinal crack: (40+10) min heating + cooling - IR camera spectral band/thermal image resolution: LWIR/640x480 pixels - Camera-to-object angle with regard to the perpendicular of the object: 0º - Thermal stimulator-to-object distance/angle with regard to the	Welding of two plaques of low carbon steel, extrapolated to infrastructure scale	Active IRT: Traditional technique of stimulation, CT, transmission mode and under laboratory conditions

	perpendicular of the object: 0.01 m/0º - Thermal image acquisition frequency: 0.2 Hz, only during the cooling		
Yang et al. [52]	- Induction heating device with a current and excitation frequency of 380 A and 256 Hz, respectively - Test campaign: Heating period is of 0.2 s (experiment 1) and 0.5 s (experiment 2) - IR camera spectral band/thermal image resolution: MWIR/320x256 pixels	Metallic rails	Active IRT: Advanced technique: eddy current/induction thermography, PT, reflection mode and under laboratory conditions
Foudazi et al. [53]	- Transmission of 50 W of power from a horn, amplified the microwave signal through a power	Metal structure	Active IRT: Advanced technique: microwave thermography, CT, reflection mode and under laboratory conditions

	amplifier unit, and with a transmission frequency of 2.4 GHz - Test campaign: optimum heating and cooling periods between 5 s @ 30 s - IR camera spectral band/thermal image resolution: LWIR/320x240 pixels - Optimum angle between the crack length and incident electric field: 0º @ 65º - Thermal image acquisition frequency: 30 Hz		
Pahlberg et al. [54]	- Ultrasonic transducer with the sonotrode in physical contact. Power/frequency of the ultrasonic wave: 1,000 W/20 kHz	Oak flooring lamellae	Active IRT: Advanced technique: ultrasound thermography, PT, reflection mode and under laboratory conditions

	- IR camera spectral band/thermal image resolution: MWIR/640x512 pixels - Camera-to-object distance/angle with regard to the perpendicular of the object: 0.6 m/0º - Thermal image acquisition frequency: 30 Hz, 300 ms after the beginning of the excitation		
López De Uralde et al. [55]	- Fibre diode laser in continuous wave mode, with plano-convex and cylindrical convergent lens to adjust the laser to the welded part and with a power interval of 10 W @ 50 W, a wavelength of 808 nm and the laser parallel to the directions of the cracks	Metallic welds, extrapolated to infrastructure scale	Active IRT: Laser thermography, CT, reflection mode and under laboratory conditions

	- Test campaign: Weld scanning moving the pieces linearly across the laser and camera (50 mm/min @ 400 mm/min) - IR camera spectral band/thermal image resolution: MWIR/640x512 pixels - Camera-to-object distance/angle with regard to the perpendicular of the object: 15 cm and 50 cm/0º - Thermal image acquisition frequency: 200 Hz		

Table 3. Comparative table of the most recent IRT works related to the analysis of cracking within civil infrastructures.

Table 4 describes four recent IRT studies that analyse subsuperficial defects within civil infrastructures.

Work [Ref.]	Experimental setup	Infrastructure under study	Type of IRT data acquisition

Rodríguez-Martín et al. [56]	- Laboratory conditions: T_{atm} at 21 ºC and RH_{atm} at 78% - Electric heater with 2,500 W - Test campaign: Continuous heating up to 70 ºC + cooling 300 s - IR camera spectral band/thermal image resolution: LWIR/640x480 pixels - Camera-to-object angle with regard to the perpendicular of the object: 0º - Thermal stimulator-to-object distance/angle with regard to the perpendicular of the object: 0.02 m/0º - Thermal image acquisition frequency: 0.2 Hz, only during the cooling	Welding of two plaques of low carbon steel, extrapolated to infrastructure scale	Active IRT: Traditional technique of stimulation, CT, reflection/transmission mode and under laboratory conditions

Xu et al. [57]	- Induction heater system with a maximum excitation power and operating current of 2.4 kW and 400 A, respectively, and with an operating excitation frequency of 195 kHz - Test campaign: Cooling period (0 to 200 ms) + heating period (201 ms to 500 ms) + cooling period (501 ms to 2400 ms) - IR camera spectral band/thermal image resolution: LWIR/320x240 pixels - Thermal image acquisition frequency: 50 Hz	Corroded steel bar	Active IRT: Advanced technique: eddy current/induction thermography, PT, reflection mode and under laboratory conditions
Ranjit et al. [58]	- Two halogen lamps, of 1 kW each, with a sinusoidal thermal	Stainless steel sample, extrapolated to infrastructure scale	Active IRT: Optical thermography, LT,

	source, driven by a power amplifier and a function generator - Test campaign: Sinusoidal heating function. Several excitation frequencies are applied, from 0.021 Hz to 0.182 Hz, four complete excitation cycles each - IR camera spectral band/thermal image resolution: LWIR/640x480 pixels - Thermal image acquisition frequency: 50 Hz		reflection mode and under laboratory conditions
Hwang et al. [59]	- Point laser beam with 92.31 mW/mm^2, propagated to the surfaces under study with a 100 mm long and 1 mm wide line, wavelength of 532 nm	Rotating wind turbine blades	Active IRT: Laser thermography, PT, reflection mode and under laboratory conditions

	- Test campaign: Thermal wave propagation is automatically scanned by an IR camera while the blades tested rotate under normal conditions - IR camera spectral band/thermal image resolution: MWIR/640x512 pixels - Camera-to-object distance/angle with regard to the perpendicular of the object: 1 m/0º - Thermal stimulator-to-object distance/angle with regard to the perpendicular of the object: 1 m/0º - Thermal image acquisition frequency: 50 Hz

Table 4. Comparative table of the most recent IRT works related to the analysis of subsuperficial defects within civil infrastructures.

Table 5 describes four recent IRT studies that analyse hotspots within civil infrastructures.

Work [Ref.]	Experimental setup	Infrastructure under study	Type of IRT data acquisition
Ullah et al. [60]	- T_{atm} from 2 ºC to 6 ºC - IR camera spectral band/thermal image resolution: LWIR/640x480 pixels - Camera-to-object distance/angle with regard to the perpendicular of the object: 5 m @ 8 m/0º - Thermal image acquisition frequency: One single thermal image	Power substations	Passive IRT: Steady conditions and from outdoor
Ahmed et al. [61]	- T_{atm} from 30 ºC to 33 ºC - IR camera spectral band/thermal image resolution: LWIR/160x120 pixels	Switch boards	Passive IRT: Steady conditions and from outdoor

	- Camera-to-object distance/angle with regard to the perpendicular of the object: 0.5 m @ 1 m/0º - Thermal image acquisition frequency: One single thermal image		
Chaudhary and Chaturvedi [62]	- T_{atm} at 16 ºC, RH_{atm} at 72% and wind velocity at 2.1 m/s (without shading of tree). T_{atm} at 25 ºC, RH_{atm} at 24% and wind velocity at 5.1 m/s (with shading of tree) - IR camera spectral band/thermal image resolution: LWIR/160x120 pixels - Thermal image acquisition frequency: One single thermal image	Strings of a solar photovoltaic array	Passive IRT: Steady conditions and from outdoor

López-Fernández et al. [63]	- Test campaign: A thermographic flight by an Unmanned Aerial Vehicle (UAV). Period between sun zenith angle of 23.5° and an hour prior to sunset. Approximated flight speed of 10 km/h and flight height of 10 m - IR camera spectral band/thermal image resolution: LWIR/384x288 pixels - Camera-to-object distance/angle with regard to the perpendicular of the object: 10 m/20º @ 25º - Thermal image acquisition frequency: 50 Hz	Photovoltaic panels	Passive IRT: Unsteady conditions and from outdoor

Table 5. Comparative table of the most recent IRT works related to the analysis of hotspots within civil infrastructures.

3.2. Heritage sites

Table 6 describes four recent IRT studies that analyse moisture within heritage sites.

Work [Ref.]	Experimental setup	Infrastructure under study	Type of IRT data acquisition
Garrido et al. [46]	- Indoor conditions: T_{atm} at 19 ºC and RH_{atm} at 40% - IR camera spectral band/thermal image resolution: LWIR/320x240 pixels - Camera-to-object distance/angle with regard to the perpendicular of the object: ≤10 m/≤ 50º - Thermal image acquisition frequency: One single thermal image	Synthetic tesserae mosaic	Passive IRT: Steady conditions and from indoor
Cadelano et al. [64]	- Test campaign: During more than one week	Fresco mural paintings in a medieval chapel	Passive IRT: Unsteady conditions and from indoor

	- IR camera spectral band/thermal image resolution: LWIR/320x240 pixels - Camera-to-object distance: 2.5 m - Thermal image acquisition frequency: 0.0011 Hz		
Georgescu et al. [65]	- Summer period. Indoor: T_{atm} from 20.2 ºC to 21.3 ºC, RH_{atm} from 74% to 86%. Outdoor: T_{atm} at 23.7 ºC, RH_{atm} from 64.3% to 67.3%. - Thermal image acquisition frequency: 1 Hz	Historical church	Passive IRT: Steady conditions and from indoor
Garrido et al. [66]	- Test campaign: Before sunrise (wall 1) and after sunset (walls 2 and 3) - IR camera spectral band/thermal image resolution: LWIR/640x480 pixels	Building built during the first half of 20th century (wall 1), a museum built in the mid-19th century (wall 2) and an 18th century cemetery (wall 3)	Passive IRT: Steady conditions and from outdoor

	- Thermal image acquisition frequency: One single thermal image		

Table 6. Comparative table of the most recent IRT works related to the analysis of moisture within heritage sites.

Table 7 describes five recent IRT studies that analyse cracking within heritage sites.

Work [Ref.]	Experimental setup	Infrastructure under study	Type of IRT data acquisition
Lagüela et al. [16]	- T_{atm} at 26 ºC and RH_{atm} at 50% - IR camera spectral band/thermal image resolution: LWIR/640x480 pixels - Camera-to-object distance: 1 m - Thermal image acquisition frequency: One single thermal image per each zone of the esplanade	Historic esplanade made up of alternating masonry blocks fixed by mortar and grout, and patches of concrete roadbed	Passive IRT: Steady conditions and from outdoor

Ibarra-Castanedo et al. [48]	- Test campaign: 3-days survey during summer with limited solar radiation and using a 2X Telescope - IR camera spectral band/thermal image resolution: LWIR/320x240 pixels - Camera-to-object distance/angle with regard to the perpendicular of the object: 44 m/0º - Thermal image acquisition frequency: 0.0167 Hz	Bell tower	Passive IRT: Unsteady conditions and from outdoor
Kilic [67]	- Thermal image acquisition frequency: One single thermal image	Historic Ottoman building	Passive IRT: Steady conditions and from indoor
Bisegna et al. [68]	- Test campaign: Before sunrise and after sunset for many days	Ancient façades of different churches	Passive IRT: Steady conditions and from outdoor

	- IR camera spectral band/thermal image resolution: LWIR/320x240 pixels - Thermal image acquisition frequency: Several times		
Sfarra et al. [69]	- Indoor conditions: T_{atm} at 6 ºC and RH_{atm} at 70% - Air heater of 10 kW with fluid outflow velocity at 0.18 m^3/s and with combustion temperature at 197 ºC - Test campaign: During winter season. Heating for 2,050 s (34.17 min) and cooling for 95 min - IR camera spectral band/thermal image resolution: LWIR/320x240 pixels	Aediculae having a precious external coating	Active IRT: Traditional technique of stimulation, CT, transmission mode and from indoor

Table 7. Comparative table of the most recent IRT works related to the analysis of cracking within heritage sites.

Table 8 describes three recent IRT studies that analyse subsuperficial defects within heritage sites.

Work [Ref.]	Experimental setup	Infrastructure under study	Type of IRT data acquisition
Sfarra et al. [69]	- Indoor conditions: T_{atm} at 6 ºC and RH_{atm} at 70% - Air heater of 10 kW with fluid outflow velocity at 0.18 m^3/s and with combustion temperature at 197 ºC - Test campaign: During winter season. Heating for 2,050 s (34.17 min) and cooling for 95 min - IR camera spectral band/thermal image resolution: LWIR/320x240 pixels	Aediculae having a precious external coating	Active IRT: Traditional technique of stimulation, CT, transmission mode and from indoor

Sfarra et al. [70]	- Indoor conditions: T_{atm} at 10 ºC, RH_{atm} at 74% - Two IR lamps of 250 W each - Test campaign: 3,600 s heating, 3,600 s cooling - IR camera spectral band/thermal image resolution: LWIR/320x240 pixels - Camera-to-object distance/angle with regard to the perpendicular of the object: 1 m/0º - Thermal stimulator-to-object distance with regard to the perpendicular of the object: 0.98 m - Thermal image acquisition frequency: 10 Hz	Mural painting	Active IRT: Optical thermography, CT, reflection mode and from indoor

Chulkov et al. [71]	- Xenon flash tube of 3.2 kJ (test 1) and a halogen lamp of 2.5 kW (test 2) - Test campaign: Heating for 5 s (test 2) - IR camera spectral band/thermal image resolution: MWIR/320x240 pixels (test 1 and 2) - Thermal stimulator-to-object distance with regard to the perpendicular of the object: 1 m (test 1) - Thermal image acquisition frequency: 15 Hz (test 2), only during the cooling	Ancient marqueteries made of fruit woods	Active IRT: Optical thermography (test 1 and 2), CT (test 2), reflection mode (test 1 and 2) and under laboratory conditions

Table 8. Comparative table of the most recent IRT works related to the analysis of subsuperfical defects within heritage sites.

Table 9 describes three recent IRT studies that search for buried structures within heritage sites.

Work [Ref.]	Experimental setup	Infrastructure under study	Type of IRT data acquisition
Lundén [72]	- Outdoor conditions: Summer - Test campaign: Acquisition from a helicopter just before midnight in one day of August - IR camera spectral band: LWIR - Camera-to-object distance: 200 m - Thermal image acquisition frequency: Several thermal images	Archaeological remains during a road construction	Passive IRT: Steady conditions and from outdoor
Puente et al. [73]	- Without direct incidence of the sun on the surfaces - IR camera spectral band/thermal image resolution: LWIR/640x480 pixels - Camera-to-object angle with regard to the perpendicular of the object: 0º	Buried structures of a Roman-era military camp	Passive IRT: Steady conditions and from outdoor

Carlomagno et al. [74]	- Halogen lamps (site 1) - IR camera spectral band/thermal image resolution: MWIR/320x240 pixels (site 1), LWIR/640x480 pixels (site 2)	Buried wall paintings (site 1) and theatre remnants (site 2)	Active IRT: Optical thermography, PT/LT and reflection mode (site 1) Optical thermography, PT and reflection mode (site 2) From outdoor

Table 9. Comparative table of the most recent IRT works related to the search of buried structures within heritage sites.

3.3. Buildings

Table 10 describes six recent IRT studies that thermally characterize materials in buildings. Specifically, the first two IRT works included focus on the calculation of the thermal diffusivity parameter, the second IRT work included also focuses on the calculation of the thermal conductivity parameter and the last four IRT works included focus on the calculation of the overall heat transfer coefficient.

Work [Ref.]	Experimental setup	Infrastructure under study	Type of IRT data acquisition

Serra et al. [75]	- Two halogen lamps of 2,500 W - Test campaign: Rectangular heating function. Initial offset (100 s), heating period (200 s), cooling down period (one of 3,796 s and the other of 7,892 s) - IR camera spectral band/thermal image resolution: LWIR/640x480 pixels - Camera-to-object distance: 0.9 m - Thermal image acquisition frequency: 0.03125 Hz	Multi-layered system containing a thin defect, made from materials commonly used in building elements	Active IRT: Optical thermography, LT, reflection mode and under laboratory conditions
Cifuentes et al. [76]	- A continuous wave laser (532 nm), whose intensity is modulated by an acousto-optic modulator. The laser power is adjusted (50mW @ 200mW) for each material in order to obtain a similar temperature rise	Thermal insulators: homogeneous polymers, paper sheets and extruded polystyrene foams; extrapolated to infrastructure scale	Active IRT: Laser thermography, LT, transmission mode and under laboratory conditions

	at the centre of the laser spot of about 10K - Test campaign: Duration between 5 min @ 10 min - IR camera spectral band/thermal image resolution: MWIR/320x256 pixels - Thermal image acquisition frequency: 300 Hz		
Tejedor et al. [79]	- Indoor conditions established according to international standards [77,78] - Temperature difference between indoor and outdoor: 7 ºC - Test campaign: 2 h @ 3 h - IR camera spectral band/thermal image resolution: LWIR/320x240 pixels	Multi-leaf walls	Passive IRT: Steady conditions and from indoor

	- Camera-to-object distance/angle with regard to the perpendicular of the object: 1.5 m/15º - Thermal image acquisition frequency: 0.0167 Hz		
Danielski & Fröling [80]	- Indoor conditions: Fluctuating between 20 ºC @ 25 ºC - Temperature difference between indoor and outdoor: 9 ºC @ 40 ºC - Test campaign: during a period of two months; total of 3 periods. At a distance of at least 0.5 m from the corners to include only laminar heat flow through the walls - IR camera spectral band/thermal image resolution: LWIR/320x240 pixels	Thick massive laminated spruce timber walls with different thicknesses	Passive IRT: Unsteady conditions and from indoor

	- Camera-to-object distance/angle with regard to the perpendicular of the object: 2 m/15º - Thermal image acquisition frequency: 2 @ 3 thermal images per day at arbitrary hours		
Albatici et al. [81]	- Outdoor conditions: 1) early in the morning, 2) overcast sky, 3) local wind speed near the walls lower than 0.5 m/s, 4) free stream wind speed in the building boundaries 24 h prior the measurements lower than 5 m/s, 5) not rainy days during the previous days and 6) low swing (less than 6 K) in the T_{atm} during the 12 h before the measurements - Temperature difference between indoor and outdoor: ≥ 15 ºC	Timber (light) and brick (heavy) structures	Passive IRT: Steady conditions and from outdoor

	- Test campaign: 3 periods equivalent to 3 year research (November-March). Total of 56 measurement surveys, 30 min per inspection - IR camera spectral band/thermal image resolution: LWIR/320x240 pixels - Camera-to-object distance/angle with regard to the perpendicular of the object: 6 m/0º		
Patel et al. [82]	- Outdoor conditions: Daytime - Temperature difference between indoor and outdoor: 10 ºC - Test campaign: 20-25 min of flying time by UAV - IR camera spectral band: LWIR	Building envelope components	Passive IRT: Steady conditions and from outdoor

	- Camera-to-object distance/angle with regard to the perpendicular of the object: Few meters (≤ 10 m)/all the directions		

Table 10. Comparative table of the most recent IRT works related to the thermal characterization of materials in buildings. Specifically, [75,76] focus on the calculation of the thermal diffusivity parameter, [76] also focuses on the calculation of the thermal conductivity parameter and [79–82] focus on the calculation of the overall heat transfer coefficient.

Table 11 describes four recent IRT studies that analyse moisture in buildings.

Work [Ref.]	Experimental setup	Infrastructure under study	Type of IRT data acquisition
Garrido et al. [46]	- Outdoor conditions: T_{atm} at 17.9 ºC and RH_{atm} at 72% - Indoor conditions: T_{atm} at 23 ºC and RH_{atm} at 50% - IR camera spectral band/thermal image resolution: LWIR/640x480 pixels	White plaster walls in different buildings (indoor) and a concrete building façade (outdoor)	Passive IRT: Steady conditions and from outdoor/indoor

	- Camera-to-object distance/angle with regard to the perpendicular of the object: ≤10 m/≤ 50º - Thermal image acquisition frequency: One single thermal image		
Edis et al. [83]	- Outdoor conditions: T_{atm} at 20.7 ºC @ 29 ºC, RH_{atm} at 42.2% @ 67.6%, wind speed 0 @ 8 km/h, indoor temperature at 21.6 ºC @ 25 ºC and indoor relative humidity at 47.9% @ 61.9% - Test campaign: From 9:30 to 18:30 - IR camera spectral band/thermal image resolution: LWIR/240x180 pixels	Adhered ceramic façade claddings	Passive IRT: Steady conditions from outdoor

	- Camera-to-object distance/angle with regard to the perpendicular of the object: 6 m/0º - Thermal image acquisition frequency: 0.00056 Hz and 0.000278 Hz		
Edis et al. [84]	- Outdoor conditions: Rainy and dry seasons - Test campaign: Throughout the day and night of several days - IR camera spectral band/thermal image resolution: LWIR/320x240 pixels	Adhered ceramic façade claddings	Passive IRT: Steady conditions and from outdoor
Garrido et al. [85]	- Indoor conditions: T_{atm} at 23 ºC and RH_{atm} at 50% - Test campaign: Beginning of the night in spring season	Building: White plaster walls in different buildings	Passive IRT: Steady conditions and from indoor

	- IR camera spectral band/thermal image resolution: LWIR/640x480 pixels - Camera-to-object distance/angle with regard to the perpendicular of the object: ≤10 m/≤ 50º - Thermal image acquisition frequency: One single thermal image		

Table 11. Comparative table of the most recent IRT works related to the analysis of moisture in buildings.

Table 12 describes two recent IRT studies that analyse cracking in buildings.

Work [Ref.]	Experimental setup	Infrastructure under study	Type of IRT data acquisition
Bauer et al. [86]	- Two IR lamps of 750 W each (reflection mode) and one IR lamp of 750 W (transmission mode)	Mortar board, extrapolated to infrastructure scale	Active IRT: Optical thermography, CT, reflection/transmission mode and under laboratory conditions

	- Test campaign: Heating for 120 min without cooling - IR camera spectral band/thermal image resolution: LWIR/320x240 pixels - Camera-to-object distance/angle with regard to the perpendicular of the object: 1.7 m/0º (reflection/transmission mode) - Thermal stimulator-to-object distance/angle with regard to the perpendicular of the object: 0.9 m/35º (reflection mode) and 0.45 m/0º (transmission mode) - Thermal image acquisition frequency: 0.0042 Hz, only during the heating

Bauer et al. [87]	- Test campaign: During 3 days without rainfall - IR camera spectral band/thermal image resolution: LWIR/320x240 pixels - Thermal image acquisition frequency: 0.0033 Hz	Masonry façade with ceramic tile	Passive IRT: Unsteady conditions and from outdoor

Table 12. Comparative table of the most recent IRT works related to the analysis of cracking in buildings.

Table 13 describes six recent IRT studies that analyse thermal bridges in buildings.

Work [Ref.]	Experimental setup	Infrastructure under study	Type of IRT data acquisition
Garrido et al. [85]	- Outdoor conditions: T_{atm} at 12 ºC and RH_{atm} at 80% - Indoor conditions: T_{atm} at 23 ºC and RH_{atm} at 50% - Test campaign: Beginning of the night in spring season	White plaster walls in different buildings (indoor) and a pink granite façade (outdoor)	Passive IRT: Steady conditions and from outdoor/indoor

	- IR camera spectral band/thermal image resolution: LWIR/640x480 pixels - Camera-to-object distance/angle with regard to the perpendicular of the object: ≤10 m/ ≤50º - Thermal image acquisition frequency: One single thermal image		
Garrido et al. [88]	- Outdoor conditions: Centre of Spain, winter season - Test campaign: Mobile inspection vehicle. The IR camera measures with a 45º angle regarding the direction of advance - Resulting field of view of the IR camera: 2.9 m x 2.9 m at 3 m	Building envelopes, from semi-detached two-storey buildings, to five-storey self-standing buildings	Passive IRT: Steady conditions and from outdoor

	distance of the surfaces under study - IR camera spectral band/thermal image resolution: LWIR/384x288 pixels - Thermal image acquisition frequency: 20 Hz		
O'Grady et al. [89]	- Laboratory conditions in the hot box tested: 25 ºC of T_{atm}, 45% of RH_{atm} and 0.1 m/s (indoor environment); -5 ºC of T_{atm}, 40% of RH_{atm} and 1.5 m/s (outdoor environment) - Test campaign: A series of thermal images of each surface under study is acquired from the indoor environment, after a few hours of steady conditions	Chamber	Passive IRT: Steady conditions and under laboratory conditions

	- IR camera spectral band/thermal image resolution: LWIR/320x240 pixels - Thermal image acquisition frequency: Several thermal images during a specific time interval		
O'Grady et al. [90]	- Laboratory conditions in the hot box tested: 25 ºC of T_{atm} and 0.1 m/s (indoor environment); -5 ºC of T_{atm} (outdoor environment) - Test campaign: Wind velocity tested in the outdoor environment (m/s): 0.5, 1.5 and 4 - IR camera spectral band/thermal image resolution: LWIR/320x240 pixels	Chamber	Passive IRT: Steady conditions and under laboratory conditions

	- Thermal image acquisition frequency: Several thermal images during a specific time interval		
Baldinelli et al. [91]	- Laboratory conditions: Hot box apparatus with controlled environment - Test campaign: Under indoor environment (hot chamber) - IR camera spectral band/thermal image resolution: LWIR/320x240 pixels - Camera-to-object distance: 1.3 m	Chamber	Passive IRT: Steady conditions and under laboratory conditions
Douguet et al. [92]	- Outdoor conditions: Several seasons (autumn/winter, mid-season and summer) - Electrical heaters of variable power (from 250 W to 1,200 W)	Internal walls of a bungalow	Active IRT: Traditional technique of stimulation, LT, reflection mode and from indoor

	- Test campaign: Square heating function. Heating/cooling periods from 10 min to 120 min. Several measurements of about 10 consecutive night-days each - IR camera spectral band/thermal image resolution: LWIR/320x256 pixels - Thermal image acquisition frequency: 50 Hz		

Table 13. Comparative table of the most recent IRT works related to the analysis of thermal bridges in buildings.

Table 14 describes four recent IRT studies that analyse air infiltration in buildings.

Work [Ref.]	Experimental setup	Infrastructure under study	Type of IRT data acquisition
Lerma et al. [93]	- Outdoor/indoor conditions (T_{atm}, RH_{atm} and wind velocity): From 11.1 ºC, 33%, 0.9 m/s to 25.6 ºC,	Room in a building	Active IRT: Optical thermography, CT, transmission mode and from indoor

	100%, 5 m/s /from 15.6 ºC, 44% to 23.6 ºC, 82% (always ΔT < 10 ºC) - IR lamp of 2,500 W - Test campaign: A cardboard sheet is located at the bottom of a roller shutter handle, pre-heated the sheet by the IR lamp for 30 s. Several days, some in the morning and some in the afternoon (16 measurements in total per day) - IR camera spectral band/thermal image resolution: LWIR/320x240 pixels - Camera-to-object angle and cardboard sheet angle with regard to the perpendicular of the object: 0º/0º (Test 1) and 90º/90º (Test 2)

	- Thermal image acquisition frequency: Test 1: 5 thermal images each 15 s (0.33 Hz) for different pressure differences: 85 Pa and 180 Pa Test 2: One thermal image per day (0.000012 Hz) for different pressure differences: 0 Pa, 25 Pa, 75 Pa, 175 Pa and 225 Pa		
Liu et al. [94]	- Outdoor/indoor conditions (T_{atm}, pressure differences and wind velocity): 22.9 ºC/31.2 ºC, 0.3 Pa and 0.56 m/s/0.41 m/s - Test campaign: During the night, while an air conditioner blows hot air from inside. Camera measures a window wall after 3 hours of air conditioner operating	Office	Passive IRT: Steady conditions and from outdoor/indoor

Kalamees et al. [95]	- During winter period - Test campaign: With the camera from inside, various tests are performed with an air temperature difference between indoors and outdoors of ≤ 20 ºC. Each test is performed twice: One under normal conditions and the other with a pressure of 50 Pa negative under the envelopes - IR camera spectral band/thermal image resolution: LWIR/320x240 pixels - Thermal image acquisition frequency: Acquisition of thermal images after the infiltration airflow have cooled the inner surface of the envelopes	Building envelopes	Passive IRT: Steady conditions and from indoor

Barreira et al. [96]	- From the end of October to the end of December. See Table 2 and 3 for more detail in the climatic conditions used [96] - Test campaign: A roller shutter handle (surface 1) and a window frame (surface 2). Several tests with 4 different levels of pressure difference are established (Pa): 0, 25, 75 and 175 (plus 225 for surface 1). A cardboard sheet is positioned between the camera and the air flow, specifically in front of the camera and parallel to the air flow. Duration of each measurement: 75 s (surface 1) and 60 s (surface 2)	Room	Passive IRT: Steady conditions and from indoor

	- IR camera spectral band/thermal image resolution: LWIR/320x240 pixels - Thermal image acquisition frequency: 1 thermal image per 15 s (0.067 Hz)

Table 14. Comparative table of the most recent IRT works related to the analysis of air infiltration in buildings.

4. Discussion

The analysis of references has led to the conclusion that there is a predominant IRT data acquisition approach for each main objective. The general relation between main objective and predominant IRT data acquisition approach is shown below:

1) Thermal characterization of materials ←→ Active IRT to calculate thermal conductivity and diffusivity, and passive IRT to calculate overall heat transfer coefficient

2) Analysis of moisture ←→ Passive IRT

3) Analysis of cracking ←→ Active IRT, passive IRT

4) Analysis of subsuperficial defects ←→ Active IRT

5) Analysis of hotspots ←→ Passive IRT

6) Search of buried structures ←→ Passive IRT and sometimes active IRT

7) Analysis of thermal bridges ←→ Passive IRT and sometimes active IRT

8) Analysis of air infiltration ←→ Passive IRT and sometimes active IRT

The most common thermal parameters calculated with IRT in infrastructure inspection are thermal diffusivity for both civil infrastructures and buildings, and thermal conductivity and overall heat transfer coefficient for buildings. The main reason for not thermally characterizing a heritage site is that the search for optimal thermal performance is not a priority. Furthermore, passive IRT is

discarded as IRT data acquisition mode for thermal conductivity and diffusivity calculation because the computation of these thermal parameters is improved under unsteady conditions. However, passive IRT is required for overall heat transfer coefficient calculation.

Regarding moisture analysis, passive IRT is used in all the types of infrastructures, given its simplicity. Nevertheless, if the objective is to detect an internal moisture, active IRT is required.

Cracking are also analysed in all the types of infrastructures, although their importance is greater in civil infrastructures, due to their high requirements of optimal structural health, and in heritage sites, due to the effect of moisture in the degree of deterioration. There is no preference in the IRT data acquisition approach when analysing cracking, although active IRT is more employed in civil infrastructures, given the better thermal contrast obtained in the thermal images. Meanwhile, passive IRT is more used in heritage sites because the conditions of urbanization in most heritage sites (isolated location, non-availability of electricity connection) only allow for the performance of passive IRT and because sudden thermal changes and high temperatures in delicate materials must be avoided.

In the case of subsuperficial defects, active IRT is required, due to the limitations of passive IRT for this task. For the same reasons as for the analysis of cracking, the most recent IRT studies regarding this defect focus on civil infrastructures and heritage sites.

It should be noted that passive IRT is the predominant IRT data acquisition approach in the particular main objectives of each type of infrastructure, even to search for buried structures in heritage sites probably due to the great difficulty in applying active IRT.

As for the infrastructures tested, heritage sites are the only type of infrastructure where samples that can be extrapolated to infrastructure scale are not analysed, being samples mostly used in civil infrastructures.

Regarding active IRT, the predominant thermal stimulators are the following:

1) Optical thermography (Civil infrastructures and Buildings) to calculate thermal diffusivity. Laser thermography (Buildings) to calculate thermal conductivity.

2) Traditional techniques (Civil infrastructures and Heritage sites), advanced techniques (Civil infrastructures), laser thermography (Civil infrastructures) and optical thermography (Buildings) to analyse cracking.

3) Traditional techniques (Heritage sites), optical thermography (Heritage sites) and all the types of thermal stimulators (Civil infrastructures) to analyse subsuperficial defects.

4) Optical thermography (Heritage sites) to search buried structures.

5) Traditional techniques (Buildings) to analyse thermal bridges.

6) Optical thermography (Buildings) to analyse air infiltration.

Analysing the previous points, traditional techniques and optical thermography are the only thermal stimulators used for heritage sites. The same techniques are used for buildings, including laser thermography. This selection is the result of the difficulties involved in applying an IRT active test to full-scale infrastructures, given their large dimensions, in addition to the conditions of urbanization in most heritage sites and the delicacy of some materials at high thermal excitation and high temperatures mentioned above. Instead, there is a great interest in applying advanced techniques in samples that can be extrapolated to an infrastructure scale and that are thermally robust in civil infrastructures.

Table 15 groups the types of heating used in each type of infrastructure, together with the corresponding thermal stimulators used, duration of heating/cooling periods and thermal image acquisition frequency.

Type of infrastructure	Predominant type of heating	Thermal stimulator	Duration of heating/cooling periods		Thermal image acquisition frequency
			Heating	Cooling	
Civil infrastructures	CT	Traditional techniques	From 1,800 s to 3,000 s	300 s	0.2 Hz
		Optical thermography	10 s	10 s	-
		Advanced techniques	From 5 s to 30 s	From 5 s to 30 s	30 Hz
		Laser thermography	-	-	200 Hz
	PT	Optical thermography	From 0.002 s to 4 s	From 19.998 s to less than 60 s	50 Hz
		Advanced techniques	From 0.2 s to 0.5 s	From 0.501 s to 2.4 s	30 Hz
		Laser thermography	-	-	50 Hz
	LT	Optical thermography	From 5.49 s to 47.62 s over four cycles (sinusoidal wave)	From 5.49 s to 47.62 s over four cycles (sinusoidal wave)	50 Hz
Heritage sites	CT	Traditional techniques	2,050 s	5,700 s	-
		Optical thermography	From 5 s to 3,600 s	3,600 s	From 10 Hz to 15 Hz
	PT	Optical thermography	-	-	-
	LT	Optical thermography	-	-	-
Buildings	CT	Optical thermography	From 30 s to 7,200 s	Duration of a morning or an afternoon	From 0.000012 Hz to 0.33 Hz
	LT	Traditional techniques	From 600 s to 7,200 s (square wave)	From 600 s to 7,200 s (square wave)	50 Hz
		Optical thermography	An initial offset (100 s), a heating period (200 s) and a cooling down period (one of 3,796 s and the other of 7,892 s) (rectangular wave)		0.03125 Hz
		Laser thermography	-	-	300 Hz

Table 15. Types of heating used in each type of infrastructure, together with the corresponding thermal stimulators used, duration of heating/cooling periods and thermal image acquisition frequency.

Analysing Table 15, the three existing types of heating are used in both civil infrastructures and heritage sites, using CT and LT only in buildings. This demonstrates the difficulty of applying PT in large structures, given its short heating time, requiring high power in the thermal stimulators. Instead, CT and LT are used in thick structures due to the longer duration of their heating, not being necessary such high power in the thermal sources, consequently avoiding the damage in delicate infrastructures. Regarding CT, a longer heating and cooling time is generally more appreciated using traditional techniques in heritage sites than in civil infrastructures. The same happens using optical thermography, being the heating/cooling durations similar when applying CT on heritage sites and buildings.

Although information on the heating/cooling durations in heritage sites is missing in both PT and LT, the same time difference between civil infrastructures and heritage sites/buildings is deduced, as heating/cooling durations in LT applied in buildings are also longer than in civil infrastructures.

It should be noted that traditional techniques are not used in PT (probably because of their low power values) and advanced techniques are used in CT and PT, with a shorter heating/cooling time compared to other types of thermal stimulators.

Regarding thermal image acquisition frequency used in active IRT studies, there is no pattern for differentiation, although there is a tendency for frequencies in PT to be higher than in CT and LT due to the different characteristic heating/cooling times.

Moreover, there is no predominant preference between reflection/transmission mode both in heritage sites and buildings, being reflection mode the predominant mode in civil infrastructures.

Regarding the location of the test, all the most recent active IRT studies in civil infrastructures are performed under laboratory conditions, while buildings are mostly inspected from indoors and heritage sites are mostly inspected both from outdoors and indoors.

As regards passive IRT, predominantly the most recent IRT studies are under steady conditions in all the types of infrastructures, although there are cases of unsteady conditions. The reason is because a steady condition is more suitable when analysing the natural thermal behaviour of a structure. There is no predominant preference between outdoor/indoor in heritage sites and buildings, being more frequent outdoor inspection in civil infrastructures. From outdoors, before sunrise and after sunset are the optimal times to test regardless of the main objective, in all the types of infrastructures. This is because there is no direct solar radiation affecting the natural thermal behaviour of the infrastructure, and the thermal stimulation due to the solar radiation is higher (i.e., more thermal contrast under steady conditions) either when it starts to heat the environment (before sunrise) or when the Sun disappears and the environment starts to cool (after sunset).

The thermal image acquisition frequency used in passive IRT works is similar among the different types of infrastructures to be analysed, from one single thermal image to around 1 Hz (one thermal image per second) when testing in a

fixed position, being the most common frequency of 20 Hz and 50 Hz by means of a mobile vehicle and an UAV, respectively.

Finally, analysing the camera-to-object distance/angle with regard to the perpendicular of the object, similar values are used in all IRT studies regardless of the type of infrastructure, IRT data acquisition approach and main objective, ranging from 0.15 m/0º to 10 m/50º. Thermal information would be lost on the thermal images acquired from distances higher than 10 m due to the low resolution of the IR cameras, and angles greater than 50º could provoke the measurement of reflections on the surface under study, obtaining erroneous temperatures of the infrastructure (0º is used in the particular case that reflection does not exist). Similar values are also used regarding the thermal stimulator-to-object distance/angle with regard to the perpendicular of the object in all the types of infrastructures, regardless the main objective, ranging from 0.01 m to 1 m/from 0º to 35º. Distances and angles with higher values may cause loss of control of the heat generated by the thermal stimulator.

Last, regarding the IR camera spectral band, the MWIR band is used in some recent IRT studies in all the types of infrastructures, especially in active IRT studies where the surface temperature exceeds 125°C, but the predominant band for all cases is the LWIR band. Thermal image resolution used is similar for all the types of infrastructures, ranging from 160x120 pixels to 640x512 pixels.

5. Conclusions

This paper develops an exhaustive review of the most recent data acquisition procedures applied with IRT in the infrastructure field. Specifically, the infrastructure and the type of infrastructure (civil infrastructures/heritage sites/buildings), experimental setup, type of IRT data acquisition (active/passive IRT) and main objective (thermal characterization of materials; moisture; cracking; subsuperficial defects; hotspots; search of buried structures; thermal bridges; air infiltration) of each recent IRT study is described.

In spite of the great heterogeneity among all the data acquisition procedures, the following points can be cited as global conclusions, both objective and critical:

- In civil infrastructures, active IRT is used to calculate the thermal diffusivity parameter and to analyse cracking and subsuperficial defects, while passive IRT is applied to analyse moisture and hotspots and to a lesser extent cracking. In heritage sites, active IRT is used to analyse subsuperficial defects and to a lesser extent to analyse cracking and search of buried structures, and passive IRT is used to analyse moisture, cracking and search of buried structures. In buildings, active IRT is used to calculate the thermal conductivity and diffusivity parameter and to analyse cracking and to a lesser extent to the analysis of thermal bridges and air infiltrations, whereas passive IRT is applied to calculate the overall heat transfer coefficient and to analyse moisture, cracking, thermal bridges and air infiltration.

- Application of IRT data acquisition procedures to a wide variety of infrastructures in both buildings and heritage sites. In civil infrastructures, the

authors encourage to test other infrastructures that are not composites, concrete, metals or electric structures, in order to continue improving this technique by offering better results.

- Regarding thermal stimulators, in civil infrastructures the traditional techniques are used to analyse cracking and subsurface defects, optical thermography to calculate thermal diffusivity and analyse subsuperficial defects and laser thermography and advanced techniques to analyse cracking and subsuperficial defects. In heritage sites, traditional techniques are used to analyse cracking and subsuperficial defects, and optical thermography to analyse subsuperficial defects and search for buried structures. In buildings, traditional techniques are used to analyse thermal bridges, optical thermography to calculate thermal diffusivity and to analyse cracking and air infiltration, and laser thermography to calculate thermal conductivity.

- The three types of heating (CT, PT and LT) are used in both civil infrastructures and heritage sites, being only CT and LT used in buildings.

- The heating/cooling durations are similar both in CT, PT and LT if an active IRT study is applied to a heritage site or a building, and generally longer than in civil infrastructures.

- Traditional techniques are not used in PT, and advanced techniques are used both in CT and PT, with shorter heating/cooling time compared to other types of thermal stimulators.

- The trend is to acquire thermal images at higher frequencies in PT than in CT and LT, although there are a significant number of IRT studies that do not provide this information.

- The choice of the type of heating will depend on the thickness of the structure under analysis and its thermal properties, in addition to the robustness of a material in the face of sudden thermal changes and high temperatures.

- There is no predominant preference between reflection/transmission mode both in heritage sites and buildings, being reflection mode the predominant mode in civil infrastructures.

- All the most recent active IRT studies in civil infrastructures are performed under laboratory conditions, while buildings are also analysed from indoors and heritage sites are also studied both from indoors and outdoors. This reflects the technical and economical complexity of applying artificial external thermal sources on a real scale. With the improvement and discovery of new equipment, it is expected that this limitation will be diminished.

- Although active IRT does not depend so much on the environmental conditions as passive IRT, the authors of this review have detected a lack of information regarding ambient conditions in active IRT works. Few recent studies applying active IRT included in this work provide information about ambient conditions, although there is more information on ambient conditions in works applied to heritage sites and buildings than in works about civil infrastructures. This information should be provided mainly when experimenting in transmission mode, since in that case the surface studied is not directly

affected by the artificial thermal source and environmental conditions play a role.

- In passive IRT, steady conditions predominate with regard to unsteady conditions because, although the inspection can be outdoors and affected by the Sun, the thermal image acquisition time is usually very short. In addition, thermal excitation from the Sun is much lower in magnitude than the thermal excitation of an artificial external thermal stimulator. These facts make that environmental changes, and changes in the infrastructure, are so slow that can be considered negligible.

- Following the previous point, the optimal hour for experiments outdoors and in passive IRT is either before sunrise or after sunset, regardless the type of infrastructure and main objective. In addition, it is recommended that all outdoor passive IRT studies avoid rain so that wet surfaces are not erroneously considered as defects.

- The thermal image acquisition frequency is similar among the different types of infrastructures when a passive IRT study is performed, being lower regarding the frequency value used in active IRT studies, although there is a significant number of IRT studies that do not provide this information. This parameter is especially important when a mobile platform is used, where the frequency values of passive IRT studies are similar to those used in active IRT studies.

- The camera-to-object distance/angle with regard to the perpendicular of the object is similar in all IRT studies regardless of the type of infrastructure, IRT

data acquisition approach and main objective, although there is a significant number of IRT studies that do not provide this information.

- The thermal stimulator-to-object distance/angle with regard to the perpendicular of the object is similar in all IRT studies regardless of the type of infrastructure and main objective, although there is a significant number of IRT studies that do not provide this information.

- The MWIR band is used in some recent IRT studies in all the types of infrastructures, especially in active IRT studies where the surface temperature exceeds 125°C. For all the other types of studies, the predominant band is the LWIR band.

- A similar thermal image resolution is used in all the types of infrastructures, being the technology available the cause for this selection.

- In economic and feasibility terms, passive IRT should always be preferred with respect to active IRT for all types of infrastructures, especially in the case of in situ inspections of very large structures. The only exception is the analysis of subsuperficial defects, where active IRT is the only valid IRT data acquisition mode.

- A standard IRT data acquisition protocol is needed for each type of infrastructure, and even for each type, according to the type of IRT data acquisition and main objective, in order to achieve the maximum possible efficiency and performance.

Acknowledgements

Authors would like to thank the Ministerio de Economía y Competitividad (Gobierno de España) for the financial support given through programs for human resources (FPU16/03950). Special thanks to the Cátedra Iberdrola VIII Centenario – University of Salamanca for funding given to personnel resources. This project has received funding from the European Union's Horizon 2020 research and innovation programme under grant agreement No 769255. This document reflects only the author's view and the European Commission is not responsible for any use that may be made of the information it contains.

References

[1] Strategic Infrastructure 2014 - Reports - World Economic Forum, (2014). https://www.weforum.org/reports/strategic-infrastructure-2014.

[2] P.C. Chang, A. Flatau, S.C. Liu, Review Paper: Health Monitoring of Civil Infrastructure, Struct. Heal. Monit. 2 (2003) 257–267. doi:10.1177/1475921703036169.

[3] S. Dorafshan, M. Maguire, Bridge inspection: human performance, unmanned aerial systems and automation, J. Civ. Struct. Heal. Monit. 8 (2018) 443–476. doi:10.1007/s13349-018-0285-4.

[4] K.L. Rens, T.J. Wipf, F.W. Klaiber, Review of Nondestructive Evaluation Techniques of Civil Infrastructure, J. Perform. Constr. Facil. 11 (1997) 152–160. doi:10.1061/(ASCE)0887-3828(1997)11:4(152).

[5] F. Khodayar, S. Sojasi, X. Maldague, IRT for NDT: 2050 Horizon, in: Proc. 2015 Asia Int. Conf. Quant. InfraRed Thermogr., QIRT Council,

2015. doi:10.21611/qirt.2015.0001.

[6] M. Miskiewicz, J. Lachowicz, P. Tysiac, P. Jaskula, K. Wilde, The application of non-destructive methods in the diagnostics of the approach pavement at the bridges, in: IOP Conf. Ser. Mater. Sci. Eng., 2018: p. 356:012023. doi:10.1088/1757-899X/356/1/012023.

[7] B. Riveiro, M. Solla, Non-destructive techniques for the evaluation of structures and infrastructure, CRC Press: Boca Raton, FL, USA, 2016.

[8] American Society for Nondestructive Testing, Introduction to Nondestructive Testing, (n.d.). https://www.asnt.org/MinorSiteSections/AboutASNT/Intro-to-NDT (accessed June 28, 2019).

[9] H.J. Heather-Smith, A. Smith, N. Dixon, J.A. Flint, Monitoring buried infrastructure deformation using acoustic emissions, in: 9th Eur. Work. Struct. Heal. Monit., Manchester, England, 2018.

[10] Y. Sun, S. Liu, Z. Deng, R. Tang, W. Ma, X. Tian, Y. Kang, L. He, Magnetic flux leakage structural health monitoring of concrete rebar using an open electromagnetic excitation technique, Struct. Heal. Monit. 17 (2018) 121–134. doi:10.1177/1475921716684340.

[11] M. Evans, A. Lucas, I. Ingram, The inspection of level crossing rails using guided waves, Constr. Build. Mater. 179 (2018) 614–618. doi:10.1016/j.conbuildmat.2018.05.178.

[12] F.J. Prego, L. Nieto, M. Solla, I. Puente, A mobile android tool for simplified GPR data processing in construction applications, Autom. Constr. 89 (2018) 170–182. doi:10.1016/j.autcon.2018.01.017.

[13] S. Sfarra, C. Ibarra-Castanedo, S. Ridolfi, G. Cerichelli, D. Ambrosini, D. Paoletti, X. Maldague, Holographic Interferometry (HI), Infrared Vision and X-Ray Fluorescence (XRF) spectroscopy for the assessment of painted wooden statues: a new integrated approach, Appl. Phys. A. 115 (2014) 1041–1056. doi:10.1007/s00339-013-7939-1.

[14] D. Buchta, C. Heinemann, G. Pedrini, C. Krekel, W. Osten, Combination of FEM simulations and shearography for defect detection on artwork, Strain. 54 (2018) e12269. doi:10.1111/str.12269.

[15] J. Martínez-Sánchez, M. Nogueira, H. González-Jorge, M. Solla, P. Arias, SITEGI Project: Applying Geotechnologies to Road Inspection. Sensor Integration and software processing, ISPRS Ann. Photogramm. Remote Sens. Spat. Inf. Sci. II-5/W2 (2013) 181–186. doi:10.5194/isprsannals-II-5-W2-181-2013.

[16] S. Lagüela, M. Solla, I. Puente, F.J. Prego, Joint use of GPR, IRT and TLS techniques for the integral damage detection in paving, Constr. Build. Mater. 174 (2018) 749–760. doi:10.1016/j.conbuildmat.2018.04.159.

[17] I. Puente, M. Solla, S. Lagüela, J. Sanjurjo-Pinto, I. Puente, M. Solla, S. Lagüela, J. Sanjurjo-Pinto, Reconstructing the Roman Site “Aquis Querquennis” (Bande, Spain) from GPR, T-LiDAR and IRT Data Fusion, Remote Sens. 10 (2018) 379. doi:10.3390/rs10030379.

[18] S. Bagavathiappan, B.B. Lahiri, T. Saravanan, J. Philip, T. Jayakumar, Infrared thermography for condition monitoring – A review, Infrared Phys. Technol. 60 (2013) 35–55. doi:10.1016/J.INFRARED.2013.03.006.

[19] E. Barreira, V.P. De Freitas, J.M.P.Q. Delgado, N.M.M. Ramos,

Thermography Applications in the Study of Buildings Hygrothermal Behaviour, InTech: Infrared Thermography, Rijeka, Croatia, 2012.

[20] A. Kylili, P.A. Fokaides, P. Christou, S.A. Kalogirou, Infrared thermography (IRT) applications for building diagnostics: A review, Appl. Energy. 134 (2014) 531–549. doi:10.1016/j.apenergy.2014.08.005.

[21] E. Lucchi, Applications of the infrared thermography in the energy audit of buildings: A review, Renew. Sustain. Energy Rev. 82 (2018) 3077–3090. doi:10.1016/j.rser.2017.10.031.

[22] V.P. Vavilov, D.D. Burleigh, Review of pulsed thermal NDT: Physical principles, theory and data processing, NDT E Int. 73 (2015) 28–52. doi:10.1016/j.ndteint.2015.03.003.

[23] R. Yang, Y. He, Optically and non-optically excited thermography for composites: A review, Infrared Phys. Technol. 75 (2016) 26–50. doi:10.1016/J.INFRARED.2015.12.026.

[24] I. Garrido, S. Lagüela, P. Arias, Infrared Thermography's Application to Infrastructure Inspections, Infrastructures. 3 (2018) 35. doi:10.3390/infrastructures3030035.

[25] I. Garrido, S. Lagüela, R. Otero, P. Arias, Thermographic methodologies used in infrastructure inspection: A review—Post-processing procedures, Appl. Energy. 266 (2020) 114857. doi:10.1016/j.apenergy.2020.114857.

[26] I. Nardi, E. Lucchi, T. de Rubeis, D. Ambrosini, Quantification of heat energy losses through the building envelope: A state-of-the-art analysis with critical and comprehensive review on infrared thermography, Build. Environ. 146 (2018) 190–205. doi:10.1016/J.BUILDENV.2018.09.050.

[27] A. Kirimtat, O. Krejcar, A review of infrared thermography for the investigation of building envelopes: Advances and prospects, Energy Build. 176 (2018) 390–406. doi:10.1016/j.enbuild.2018.07.052.

[28] R. Usamentiaga, P. Venegas, J. Guerediaga, L. Vega, J. Molleda, F. Bulnes, R. Usamentiaga, P. Venegas, J. Guerediaga, L. Vega, J. Molleda, F.G. Bulnes, Infrared Thermography for Temperature Measurement and Non-Destructive Testing, Sensors. 14 (2014) 12305–12348. doi:10.3390/s140712305.

[29] B. Wiecek, Review on thermal image processing for passive and active thermography, in: 2005 IEEE Eng. Med. Biol. 27th Annu. Conf., IEEE, 2005: pp. 686–689. doi:10.1109/IEMBS.2005.1616506.

[30] M. Solla, S. Lagüela, B. Riveiro, H. Lorenzo, Non-destructive testing for the analysis of moisture in the masonry arch bridge of Lubians (Spain), Struct. Control Heal. Monit. 20 (2013) 1366–76. doi:10.1002/stc.1545.

[31] K. Schwarz, J. Heitkötter, J. Heil, B. Marschner, B. Stumpe, The potential of active and passive infrared thermography for identifying dynamics of soil moisture and microbial activity at high spatial and temporal resolution, Geoderma. 327 (2018) 119–129. doi:10.1016/j.geoderma.2018.04.028.

[32] C. Ibarra-Castanedo, S. Sfarra, M. Klein, X. Maldague, Solar loading thermography: Time-lapsed thermographic survey and advanced thermographic signal processing for the inspection of civil engineering and cultural heritage structures, Infrared Phys. Technol. 82 (2017) 56–74. doi:10.1016/J.INFRARED.2017.02.014.

[33] F.J. Madruga, C. Ibarra-Castanedo, O.M. Conde, J.M. López-Higuera, X.

Maldague, Infrared thermography processing based on higher-order statistics, NDT E Int. 43 (2010) 661–666. doi:10.1016/j.ndteint.2010.07.002.

[34] S. Lagüela, L. Díaz-Vilariño, D. Roca, Infrared Thermography: Fundamentals and Applications, in: Non-Destructive Tech. Eval. Struct. Infrastruct., 2016: pp. 113–138. doi:10.1201/b19024-8.

[35] X. Maldague, Applications of infrared thermography in nondestructive evaluation, in: Trends Opt. Non-Destructive Test. Insp., Elsevier, 2000: pp. 591–633. doi:10.1016/B978-008043020-1/50040-5.

[36] J.M. Milne, W.N. Reynolds, The Non-Destructive Evaluation Of Composites And Other Materials By Thermal Pulse Video Thermography, in: SPIE 0520, Thermosense VII Therm. Infrared Sens. Diagnostics Control, 1985. doi:10.1117/12.946141.

[37] P. Daponte, F. Maceri, R.S. Olivito, Frequency-domain analysis of ultrasonic pulses for the measure of damage growth in structural materials, in: IEEE Symp. Ultrason., IEEE, Honolulu, HI, USA, 1990: pp. 1113–1118. doi:10.1109/ULTSYM.1990.171535.

[38] R.E. Martin, A.L. Gyekenyesi, S.M. Shepard, Interpreting the results of pulsed thermography data, Mater. Eval. 61 (2003) 611–616.

[39] F. Mercuri, U. Zammit, N. Orazi, S. Paoloni, M. Marinelli, F. Scudieri, Active infrared thermography applied to the investigation of art and historic artefacts, J. Therm. Anal. Calorim. 104 (2011) 475–485. doi:10.1007/s10973-011-1450-8.

[40] C. Ibarra-Castanedo, N.P. Avdelidis, X. Maldague, Qualitative and

quantitative assessment of steel plates using pulsed phase thermography, Mater. Eval. 63 (2005) 1128–1133.

[41] M. Streza, D. Dadarlat, Y. Fedala, S. Longuemart, Depth estimation of surface cracks on metallic components by means of lock-in thermography, Rev. Sci. Instrum. 84 (2013) 074902. doi:10.1063/1.4813744.

[42] P. Venegas, J. Perán, R. Usamentiaga, I. Sáez de Ocáriz, Projected thermal diffusivity analysis for thermographic nondestructive inspections, Int. J. Therm. Sci. 124 (2018) 251–262. doi:10.1016/J.IJTHERMALSCI.2017.10.010.

[43] D. Balageas, J.-M. Roche, Taking into account heat losses in front-face pulse IR thermography experiment for thermal diffusivity identification, in: 14th Quant. InfraRed Thermogr. Conf., Berlin, Germany, 2018: pp. 722–731. doi:10.21611/qirt.2018.082.

[44] S.-O. Gnessougou, N. Poulin, C.I. Castanedo, X. Maldague, A. De Champlain, É. Robert, Thermal Diffusivity Measurements With Flash Method at Different Depths In a Burned Composite Material, in: 14th Quant. InfraRed Thermogr. Conf., Berlin, Germany, 2018: pp. 159–167. doi:10.21611/qirt.2018.p40.

[45] V. Kalyanavalli, T.K.A. Ramadhas, D. Sastikumar, Determination of thermal diffusivity of Basalt fiber reinforced epoxy composite using infrared thermography, Meas. J. Int. Meas. Confed. 134 (2019) 673–678. doi:10.1016/j.measurement.2018.11.004.

[46] I. Garrido, S. Lagüela, S. Sfarra, F.J. Madruga, P. Arias, Automatic

detection of moistures in different construction materials from thermographic images, J. Therm. Anal. Calorim. (2019) 1–20. doi:10.1007/s10973-019-08264-y.

[47] P.M. Bach, J.K. Kodikara, Reliability of Infrared Thermography in Detecting Leaks in Buried Water Reticulation Pipes, IEEE J. Sel. Top. Appl. Earth Obs. Remote Sens. 10 (2017) 4210–4224. doi:10.1109/JSTARS.2017.2708817.

[48] E. Barreira, R.M.S.F. Almeida, M. L. Simões, D. Rebelo, Quantitative Infrared Thermography to Evaluate the Humidification of Lightweight Concrete, Sensors. 20 (2020) 1664. doi:10.3390/s20061664.

[49] M. Solla, S. Lagüela, N. Fernández, I. Garrido, Assessing rebar corrosion through the combination of nondestructive GPR and IRT methodologies, Remote Sens. 11 (2019) 1705. doi:10.3390/rs11141705.

[50] M. Solla, S. Lagüela, H. González-Jorge, P. Arias, Approach to identify cracking in asphalt pavement using GPR and infrared thermographic methods: Preliminary findings, NDT E Int. 62 (2014) 55–65. doi:10.1016/J.NDTEINT.2013.11.006.

[51] M. Rodríguez-Martín, S. Lagüela, D. González-Aguilera, J. Martínez, Thermographic test for the geometric characterization of cracks in welding using IR image rectification, Autom. Constr. 61 (2016) 58–65. doi:10.1016/J.AUTCON.2015.10.012.

[52] R. Yang, Y. He, B. Gao, G.Y. Tian, J. Peng, Lateral heat conduction based eddy current thermography for detection of parallel cracks and rail tread oblique cracks, Measurement. 66 (2015) 54–61.

doi:10.1016/J.MEASUREMENT.2015.01.024.

[53] A. Foudazi, A. Mirala, M.T. Ghasr, K.M. Donnell, Active Microwave Thermography for Nondestructive Evaluation of Surface Cracks in Metal Structures, IEEE Trans. Instrum. Meas. 68 (2019) 576–585. doi:10.1109/TIM.2018.2843601.

[54] T. Pahlberg, M. Thurley, D. Popovic, O. Hagman, Crack detection in oak flooring lamellae using ultrasound-excited thermography, Infrared Phys. Technol. 88 (2018) 57–69. doi:10.1016/J.INFRARED.2017.11.007.

[55] P. López De Uralde, E. Gorostegui-Colinas, A. Muniategui, I. Gorosmendi, B. Hériz, M. Ayuso, X. Sabalza, A new method for surface crack detection by laser thermography based on Thermal Barrier effect, in: 14th Quant. InfraRed Thermogr. Conf., Berlin, Germany, 2018: pp. 828–838. doi:10.21611/qirt.2018.105.

[56] M. Rodríguez-Martin, S. Lagüela, D. González-Aguilera, P. Arias, Cooling analysis of welded materials for crack detection using infrared thermography, Infrared Phys. Technol. 67 (2014) 547–554. doi:10.1016/J.INFRARED.2014.09.025.

[57] C. Xu, N. Zhou, J. Xie, X. Gong, G. Chen, G. Song, Investigation on eddy current pulsed thermography to detect hidden cracks on corroded metal surface, NDT E Int. 84 (2016) 27–35. doi:10.1016/J.NDTEINT.2016.07.002.

[58] S. Ranjit, K. Kang, W. Kim, Investigation of Lock-in Infrared Thermography for Evaluation of Subsurface Defects Size and Depth, Int. J. Precis. Eng. Manuf. 16 (2015) 2255–2264. doi:10.1007/s12541-015-

0290-z.

[59] S. Hwang, Y.-K. An, H. Sohn, Continuous-wave line laser thermography for monitoring of rotating wind turbine blades, Struct. Heal. Monit. 18 (2019) 1010–1021. doi:10.1177/1475921718771709.

[60] I. Ullah, F. Yang, R. Khan, L. Liu, H. Yang, B. Gao, K. Sun, Predictive Maintenance of Power Substation Equipment by Infrared Thermography Using a Machine-Learning Approach, Energies. 10 (2017) 1987. doi:10.3390/en10121987.

[61] M.M. Ahmed, A.S.N. Huda, N.A. Mat Isa, Recursive construction of output-context fuzzy systems for the condition monitoring of electrical hotspots based on infrared thermography, Eng. Appl. Artif. Intell. 39 (2015) 120–131. doi:10.1016/j.engappai.2014.11.010.

[62] A.S. Chaudhary, D.K. Chaturvedi, Observing Hotspots and Power Loss in Solar Photovoltaic Array Under Shading Effects Using Thermal Imaging Camera, Int. J. Electr. Mach. Drives. 3 (2017) 15–23.

[63] L. López-Fernández, S. Lagüela, J. Fernández, D. González-Aguilera, Automatic Evaluation of Photovoltaic Power Stations from High-Density RGB-T 3D Point Clouds, Remote Sens. 9 (2017) 631. doi:10.3390/rs9060631.

[64] G. Cadelano, P. Bison, A. Bortolin, G. Ferrarini, F. Peron, M. Girotto, M. Volinia, Monitoring of historical frescoes by timed infrared imaging analysis, Opto-Electronics Rev. 23 (2015) 102–108. doi:10.1515/oere-2015-0012.

[65] M.S. Georgescu, C.V. Ochinciuc, E.S. Georgescu, I. Colda, Heritage and

Climate Changes in Romania: The St. Nicholas Church of Densus, from Degradation to Restoration, in: Energy Procedia, Elsevier Ltd, 2017: pp. 76–85. doi:10.1016/j.egypro.2017.09.374.

[66] I. Garrido, S. Lagüela, S. Sfarra, M. Solla, ALGORITHMS FOR THE AUTOMATIC DETECTION AND CHARACTERIZATION OF PATHOLOGIES IN HERITAGE ELEMENTS FROM THERMOGRAPHIC IMAGES, (2019). doi:10.5194/isprs-archives-XLII-2-W15-497-2019.

[67] G. Kilic, Using advanced NDT for historic buildings: Towards an integrated multidisciplinary health assessment strategy, J. Cult. Herit. 16 (2015) 526–535. doi:10.1016/J.CULHER.2014.09.010.

[68] F. Bisegna, D. Ambrosini, D. Paoletti, S. Sfarra, F. Gugliermetti, A qualitative method for combining thermal imprints to emerging weak points of ancient wall structures by passive infrared thermography – A case study, J. Cult. Herit. 15 (2014) 199–202. doi:10.1016/J.CULHER.2013.03.006.

[69] S. Sfarra, Y. Yao, H. Zhang, S. Perilli, M. Scozzafava, N.P. Avdelidis, X.P.V. Maldague, Precious walls built in indoor environments inspected numerically and experimentally within long-wave infrared (LWIR) and radio regions, J. Therm. Anal. Calorim. 137 (2019) 1083–1111. doi:10.1007/s10973-019-08005-1.

[70] S. Sfarra, C. Ibarra-Castanedo, M. Tortora, L. Arrizza, G. Cerichelli, I. Nardi, X. Maldague, Diagnostics of wall paintings: A smart and reliable approach, J. Cult. Herit. 18 (2016) 229–241. doi:10.1016/j.culher.2015.07.011.

[71] A.O. Chulkov, S. Sfarra, N. Saeed, J. Peeters, C. Ibarra-Castanedo, G. Gargiulo, G. Steenackers, X.P.V. Maldague, M.A. Omar, V. Vavilov, Evaluating quality of marquetries by applying active IR thermography and advanced signal processing, J. Therm. Anal. Calorim. (2020) 1–14. doi:10.1007/s10973-020-09326-2.

[72] B. Lundén, Aerial Thermography: A Remote Sensing Technique Applied to Detection of Buried Archaeological Remains at a Site in Dalecarlia, Sweden, Geogr. Ann. Ser. A, Phys. Geogr. 67 (1985) 161–166. doi:10.2307/520479.

[73] I. Puente, M. Solla, S. Lagüela, J. Sanjurjo-Pinto, Reconstructing the Roman Site “Aquis Querquennis” (Bande, Spain) from GPR, T-LiDAR and IRT Data Fusion, Remote Sens. 10 (2018) 379. doi:10.3390/rs10030379.

[74] G.M. Carlomagno, R. Di Maio, M. Fedi, C. Meola, Integration of infrared thermography and high-frequency electromagnetic methods in archaeological surveys, J. Geophys. Eng. 8 (2011) S93–S105. doi:10.1088/1742-2132/8/3/s09.

[75] C. Serra, A. Tadeu, N. Simões, Numerical applications for experimental IRT in defective multilayered building systems, in: 14th Quant. InfraRed Thermogr. Conf., Berlin, Germany, 2018: pp. 376–378. doi:10.21611/qirt.2018.024.

[76] Á. Cifuentes, A. Mendioroz, A. Salazar, Simultaneous measurements of the thermal diffusivity and conductivity of thermal insulators using lock-in infrared thermography, Int. J. Therm. Sci. 121 (2017) 305–312. doi:10.1016/j.ijthermalsci.2017.07.023.

[77] Interim Guidelines for Thermographic Inspections of Buildings - RESNET, 2012. https://www.resnet.us/articles/resnet-revises-interim-guidelines-for-thermographic-inspections-of-buildings/ (accessed July 2, 2019).

[78] G.C. Holst, Common sense approach to thermal imaging, JCD Pub., 2000.

[79] B. Tejedor, M. Casals, M. Gangolells, X. Roca, Quantitative internal infrared thermography for determining in-situ thermal behaviour of façades, Energy Build. 151 (2017) 187–197. doi:10.1016/J.ENBUILD.2017.06.040.

[80] I. Danielski, M. Fröling, I. Danielski, M. Fröling, In Situ Measurements of Thermal Properties of Building Fabrics Using Thermography under Non-Steady State Heat Flow Conditions, Infrastructures. 3 (2018) 20. doi:10.3390/infrastructures3030020.

[81] R. Albatici, A.M. Tonelli, M. Chiogna, A comprehensive experimental approach for the validation of quantitative infrared thermography in the evaluation of building thermal transmittance, Appl. Energy. 141 (2015) 218–228. doi:10.1016/J.APENERGY.2014.12.035.

[82] D. Patel, J.E. Schmiedt, M. Röger, B. Hoffschmidt, Approach for external measurements of the heat transfer coefficient (U-value) of building envelope components using UAV based infrared thermography, in: 14th Quant. InfraRed Thermogr. Conf., Berlin, Germany, 2018: pp. 379–386. doi:10.21611/qirt.2018.026.

[83] E. Edis, I. Flores-Colen, J. de Brito, Quasi-quantitative infrared thermographic detection of moisture variation in facades with adhered

ceramic cladding using principal component analysis, Build. Environ. 94 (2015) 97–108. doi:10.1016/J.BUILDENV.2015.07.027.

[84] E. Edis, I. Flores-Colen, J. de Brito, Passive thermographic detection of moisture problems in façades with adhered ceramic cladding, Constr. Build. Mater. 51 (2014) 187–197. doi:10.1016/j.conbuildmat.2013.10.085.

[85] I. Garrido, S. Lagüela, P. Arias, Autonomous thermography: towards the automatic detection and classification of building pathologies, in: 14th Quant. InfraRed Thermogr. Conf., Berlin, Germany, 2018: pp. 359–368. doi:10.21611/qirt.2018.022.

[86] E. Bauer, E. Pavón, E. Barreira, E.K. De Castro, Analysis of building facade defects using infrared thermography: Laboratory studies, J. Build. Eng. 6 (2016) 93–104. doi:10.1016/j.jobe.2016.02.012.

[87] E. Bauer, P.M. Milhomem, L.A.G. Aidar, Evaluating the damage degree of cracking in facades using infrared thermography, J. Civ. Struct. Heal. Monit. 8 (2018) 517–528. doi:10.1007/s13349-018-0289-0.

[88] I. Garrido, S. Lagüela, P. Arias, J. Balado, Thermal-based analysis for the automatic detection and characterization of thermal bridges in buildings, Energy Build. 158 (2018) 1358–1367. doi:10.1016/J.ENBUILD.2017.11.031.

[89] M. O'Grady, A.A. Lechowska, A.M. Harte, Infrared thermography technique as an in-situ method of assessing heat loss through thermal bridging, Energy Build. 135 (2017) 20–32. doi:10.1016/J.ENBUILD.2016.11.039.

[90] M. O'Grady, A.A. Lechowska, A.M. Harte, Quantification of heat losses

through building envelope thermal bridges influenced by wind velocity using the outdoor infrared thermography technique, Appl. Energy. 208 (2017) 1038–1052. doi:10.1016/J.APENERGY.2017.09.047.

[91] G. Baldinelli, F. Bianchi, A. Rotili, D. Costarelli, M. Seracini, G. Vinti, F. Asdrubali, L. Evangelisti, A model for the improvement of thermal bridges quantitative assessment by infrared thermography, Appl. Energy. 211 (2018) 854–864. doi:10.1016/J.APENERGY.2017.11.091.

[92] R. Douguet, T.-T. Ha, V. Feuillet, J. Meulemans, L. Ibos, A novel experimental method for the in situ detection of thermal bridges in building envelopes based on active infrared thermography and singular value decomposition analysis, in: 14th Quant. InfraRed Thermogr. Conf., Berlin, Germany, 2018: pp. 396–402. doi:10.21611/qirt.2018.029.

[93] C. Lerma, E. Barreira, R.M.S.F. Almeida, A discussion concerning active infrared thermography in the evaluation of buildings air infiltration, Energy Build. 168 (2018) 56–66. doi:10.1016/j.enbuild.2018.02.050.

[94] W. Liu, X. Zhao, Q. Chen, A novel method for measuring air infiltration rate in buildings, Energy Build. 168 (2018) 309–318. doi:10.1016/J.ENBUILD.2018.03.035.

[95] T. Kalamees, Ü. Alev, M. Pärnalaas, Air leakage levels in timber frame building envelope joints, Build. Environ. 116 (2017) 121–129. doi:10.1016/J.BUILDENV.2017.02.011.

[96] E. Barreira, R.M.S.F. Almeida, M. Moreira, An infrared thermography passive approach to assess the effect of leakage points in buildings, Energy Build. 140 (2017) 224–235. doi:10.1016/J.ENBUILD.2017.02.009.